Available online at www.sciencedirect.com

SciVerse ScienceDirect

Ceramics International 38 (2012) 2395–2402

CERAMICS INTERNATIONAL

www.elsevier.com/locate/ceramint

Non-isothermal crystallization kinetics and microstructure of a silver doped calcium aluminophosphate glass

S. Banijamali [a,*], A.R. Aghaei [a], B. Eftekhari Yekta [b]

[a] Ceramic Division, Materials & Energy Research Center, Tehran, Iran

[b] Ceramic Division, Materials Engineering Department, Iran University of Science & Technology, Tehran, Iran

Received 4 August 2011; received in revised form 28 October 2011; accepted 2 November 2011

Available online 7 November 2011

Abstract

The role of metallic silver in crystallization behavior of $CaO–Al_2O_3–TiO_2–P_2O_5$ system glasses was investigated utilizing differential thermal analysis, X-ray diffractometry, atomic force microscope and scanning electron microscopy. Initial glasses were heat treated in hydrogen atmosphere to convert silver ions to the metallic state, prior to crystallization. The presence of metallic silver led to noticeable decreasing of crystallization temperatures as well as effective crystallization of calcium titanium phosphate ($CaTi_4(PO_4)_6$), calcium metaphosphate ($Ca(PO_3)_2$) and calcium pyrophosphate ($Ca_2P_2O_7$) phases. Kinetic of crystallization was also evaluated before and after hydrogen heat treatment under non-isothermal conditions. It was found that activation energy for crystallization was not significantly influenced by the metallic silver. However, the calculated Avrami exponents confirmed the dominant role of metallic silver as an effective nucleating agent in bulk crystallization of the reduced glasses. By leaching of the silver free and silver containing glass–ceramics, calcium pyrophosphate ($Ca_2P_2O_7$) phase was selectively dissolved out and left porous microstructures with various pore morphologies and dimensions.

Keywords: Metallic silver; Crystallization; Kinetic measurements

1. Introduction

Porous glass–ceramics based on the $CaO–TiO_2–P_2O_5$ system were first introduced by Hosono in 1989 [1,2]. Crystallization of two crystalline phases ($Ca_3(PO_4)_2$ and $CaTi_4(PO_4)_6$), which have different chemical resistance against acidic solutions, provides possibility to obtain porous glass–ceramics due to the selective dissolution of $Ca_3(PO_4)_2$ during acid leaching [1,2]. Hosono et al. could induce different properties such as ionic conductivity [3,4], antibacterial behavior [5,6] and catalytic activity [7,8] by addition of various oxides to the prototype glass system. Recently, some attempts have been reported on improving of mechanical strength, chemical resistance and self-cleaning ability of the aforementioned glass–ceramics [9,10].

In spite of these varieties in compositions and properties, restricted glass-forming region and surface crystallization affinity are the main drawbacks of the relevant glass–ceramics [1,2]. Limited efforts have been focused on improving of glass-forming ability by modification of the primary system to the $CaO–Al_2O_3–TiO_2–P_2O_5$ system [11]. The results were extended glass-forming region as well as keeping the possibility to achieve porous structures after leaching.

In a previous work [12], the present authors have investigated the role of ionic and metallic silvers in crystallization behavior of $CaO–Al_2O_3–TiO_2–P_2O_5$ glasses in order to overcome surface crystallization tendency. It was found that appropriate amounts of metallic silver can change crystallization behavior, positively.

The present work aims to find the crystallization mechanism of the as mentioned glasses in the presence of ionic and metallic silver under non-isothermal conditions. In this regard, silver free and silver containing glasses belonging to the $CaO–Al_2O_3–TiO_2–P_2O_5$ system were fabricated. A reducing heat treatment in hydrogen atmosphere was carried out to convert Ag^+ ions to the metallic state (Ag^0). Phase evolution of both glass series was evaluated through subsequent crystallization heat treatment in air atmosphere. The activation energy for crystallization and the

* Corresponding author. Tel.: +98 9122132080; fax: +98 2616201888.
E-mail address: banijamalis@yahoo.com (S. Banijamali).

0272-8842/$36.00
doi:10.1016/j.ceramint.2011.11.005

Avrami exponents were calculated as the kinetic parameters. The microstructures of the silver free and silver containing glass–ceramics were also examined.

2. Experimental procedure

Glass samples with composition of 19CaO, $9Al_2O_3$, $11.5TiO_2$, $60.5P_2O_5$ (wt.%) were prepared as the blank specimens (G0 series). Silver containing glasses (G3 series) were fabricated by addition of 3 weight parts of silver to the G0 composition. The starting materials were reagent-grade chemicals of calcium carbonate (Merck 2066), silver chloride (Merck 12330), aluminum oxide (Merck 1092), titanium oxide (BDH 30446) and phosphorus oxide (Merck 540). The homogenized mixtures of these materials were melted in alumina crucibles at the temperature interval of 1380–1420 °C in an electric furnace for 4 h. The melts were cast in a preheated graphite mould. The shaped glasses were first annealed at 500 °C for 1 h in air atmosphere and then allowed to cool naturally to room temperature. Bulk glasses were cut and polished to reach glass bars with dimension of 10 mm × 10 mm × 3 mm. In order to reduce silver ions to the metallic state, silver containing annealed glasses were also exposed to an additional heat treatment in hydrogen atmosphere at 500 °C for 3 h under hydrogen flow of 150 cm^3/min. The precipitated silver particles in the reduced series were monitored by atomic force microscope (AFM) (DualScope™ C-26) in the non-contact mode. Polished and hydrogen treated surface of the glasses was exposed to a scanning probe with tip radius of 15 nm. Thermal behavior of the glasses was investigated by differential thermal analyzer (DTA) (Polymer Laboratories, STA-1640) at a heating rate of 10 °C/min in air atmosphere. Alumina was used as the reference material and the condition of atmosphere control was static. Each DTA run was performed on sample with particle size of 0.5–0.6 mm. To ensure complete reduction of silver ions in the reduced glasses, the same sized glass particles were reduced in hydrogen atmosphere prior to the DTA analysis.

To obtain kinetic parameters, DTA thermographs of the silver containing glasses before and after reduction were recorded at the heating rates of 5, 10, 15 and 20 °C/min. Activation energy for crystallization was calculated from Eq. (2-1) according to the Marotta method [13]:

$$\ln \alpha = -\frac{E}{RT_C} + \text{Const.} \tag{2-1}$$

The Avrami exponents of the untreated and hydrogen treated silver bearing glasses were extracted from Eqs. (2-2) and (2-3) according to the Marotta and the Ozawa methods, respectively [13–16]:

$$\ln \Delta T = -\frac{nE}{RT} + \text{Const.} \tag{2-2}$$

$$\ln[-\ln(1-x)] = -n \ln \alpha + \text{Const.} \tag{2-3}$$

where α, R, T_C, ΔT, x, E and n are referred to the heating rate, gas constant, crystallization temperature, deviation from the baseline, volume fraction of crystallization, activation energy for crystallization and the Avrami exponent, accordingly.

The crystalline phases of the heat treated specimens were identified by X-ray diffractometer (XRD) (Siemens, D500). Scanning electron microscope (SEM) (Vega-Tescan) was used to examine the microstructure of the leached glass–ceramics. Leaching was performed by immersing the bulk glass–ceramics in 1 N HNO_3 solution at room temperature for 5 days.

3. Results and discussion

3.1. Differential thermal analysis

Fig. 1 shows the DTA thermographs of the silver free and silver containing glasses after air annealing. Two crystallization peaks are detectable in each DTA thermograph. According to the further XRD analysis, the first peak is attributed to the formation of calcium pyrophosphate ($Ca_2P_2O_7$) and the second peak is related to the simultaneous formation of calcium titanium phosphate ($CaTi_4(PO_4)_6$) and titanium pyrophosphate (TiP_2O_7) phases. Moreover, it can be realized from Fig. 1 that the dilatometric softening point, crystallization and liquidus temperatures of glass G3 have been decreased rather than the silver free glass. Since Ag^+ ions take part into the glass structure as the network modifiers [17,18], they could act as a fluxing agent and decrease the mentioned indicative temperatures.

Applying the reducing heat treatment in hydrogen atmosphere changed crystallization behavior of the examined glasses according to Fig. 2. A comparison between the DTA thermographs of two glass series reveals considerable changing

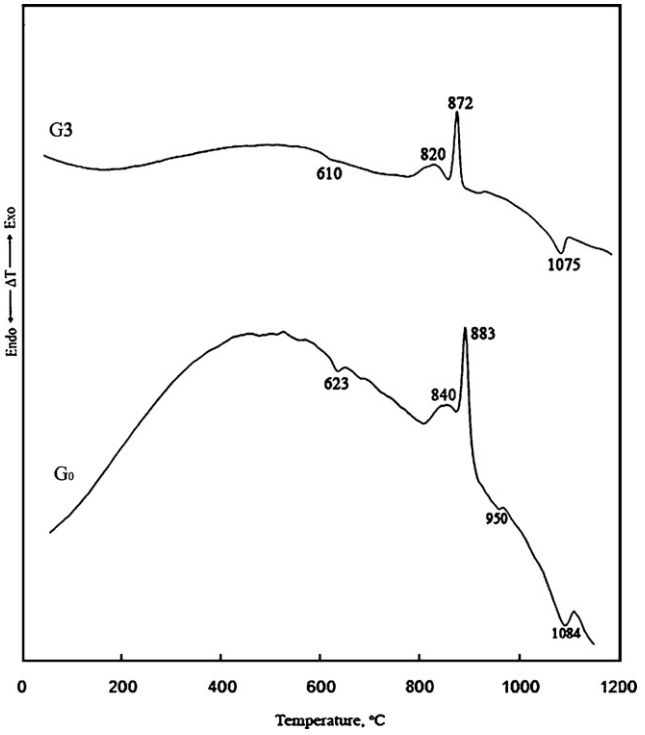

Fig. 1. DTA thermographs of 0.5–0.6 mm particles of the glasses at the heating rate of 10 °C/min before hydrogen treatment.

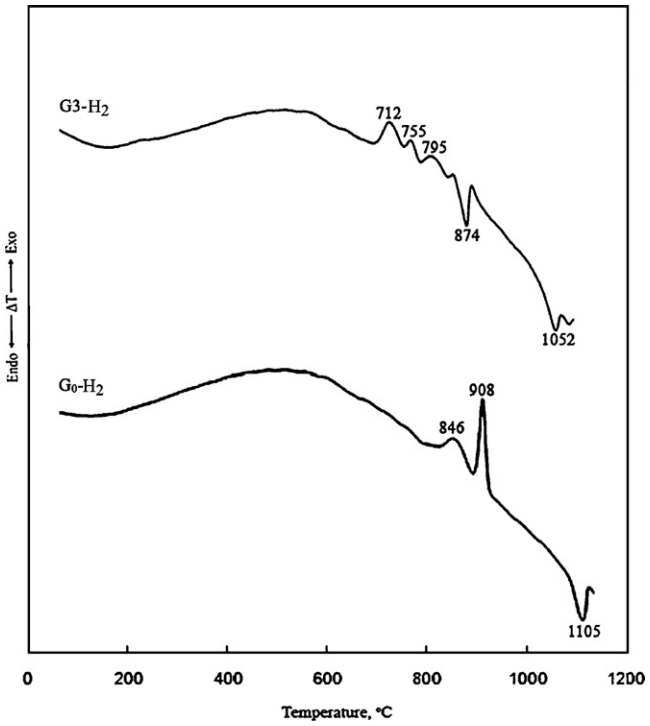

Fig. 2. DTA thermographs of 0.5–0.6 mm particles of the glasses at the heating rate of 10 °C/min after hydrogen treatment.

of crystallization trend in glass G3. Based on Fig. 2, three crystallization peak temperatures can be observed in the DTA thermograph of this glass. The crystallization temperatures have been declined as much as about 100 °C. Decreasing the crystallization temperatures was accompanied by decreasing the crystallization peak intensities. It seems that the precipitated metallic silver particles provides appropriate sites for heterogeneous nucleation of the crystalline phases and reduces crystallization temperatures, thermodynamically. On the other hand, extensive falling of the crystallization temperatures decreases the diffusion rates of necessary constituents of crystalline phases. This conditions acts against crystallization as a kinetic barrier and probably is responsible for decreasing of the peak intensities of glass G3.

As it was expected, the indicative temperatures of glass G0 were shifted to the higher temperatures after reduction. It should be noted that changing of Ti^{4+} and P^{5+} ions into Ti^{3+} and P^{3+} ions may be possible through reducing heat treatment [1,19]. Subsequently, the number of non-bridging oxygen will be reduced to keep electrical neutrality of the glass structure. As a result, the glass viscosity will be increased and the indicative temperatures will be transferred to the higher temperatures.

3.2. X-ray diffraction analysis

Fig. 3 shows the XRD patterns of the as-received powdered glasses (0.5–0.6 mm) after 5 min heat treatment at the first (p1) and the second (p2) crystallization peak temperatures. It was found that the same crystalline phases, i.e. calcium pyrophosphate, calcium titanium phosphate and titanium pyrophosphate, have been crystallized in both

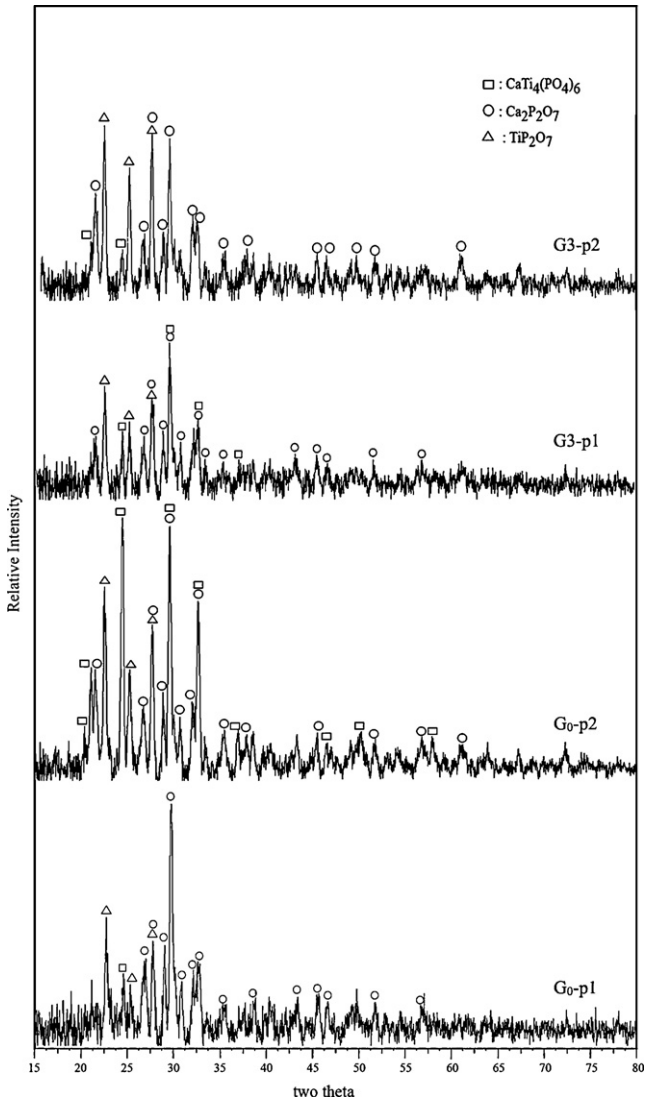

Fig. 3. XRD patterns of glasses' powders heat treated for 5 min at their crystallization peak temperatures.

glasses. According to the previous work [11], calcium pyrophosphate and titanium pyrophosphate are crystallized at the first and the second crystallization peak temperatures, respectively through surface crystallization mechanism; whilst, crystallization of calcium titanium phosphate occurs at the second crystallization peak temperature, voluminously. No silver bearing crystalline phase was detected in the XRD pattern of glass G3. Fig. 4 depicts the XRD patterns of the reduced particles (0.5–0.6 mm) of glass G3 before and after heat treatment at its crystallization peak temperatures. According to Fig. 4, some peak lines of metallic silver have been appeared after heat treatment in hydrogen atmosphere. By heat treatment at the first (p1), the second (p2) and the third (p3) crystallization peak temperatures, calcium titanium phosphate, calcium metaphosphate ($Ca(PO_3)_2$) and calcium pyrophosphate were precipitated, respectively. However, titanium pyrophosphate was not detectable after crystallization. Presumably, crystallization of calcium titanium phosphate at the first crystallization peak

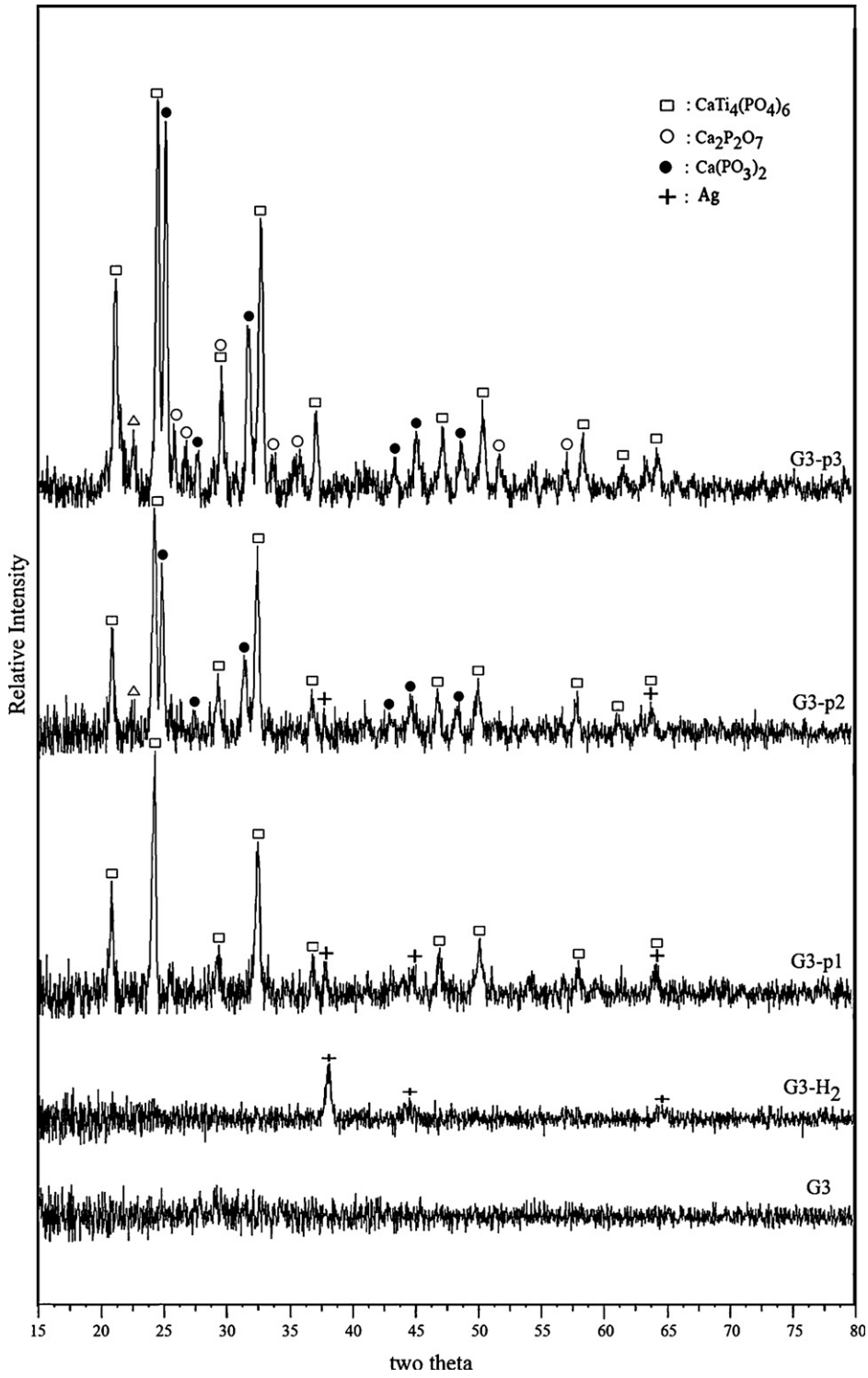

Fig. 4. XRD patterns of reduced powder of glass G3 after heat treatment at the crystallization peak temperatures.

temperature, which consumes noticeable amounts of TiO_2, enriches the residual glass phase in CaO and P_2O_5 and results in crystallization of calcium phosphate phases but not the titanium pyrophosphate.

Comparing the DTA thermographs and the XRD patterns of glass G3 before and after hydrogen heat treatment, it can be deduced that metallic silver acts as a nucleating agent and facilitates crystallization of the reduced glasses.

3.3. Kinetic measurements

To obtain a better understanding of crystallization mechanism in the presence of metallic silver, activation energy for crystallization and the Avrami exponent of glass G3 before and after hydrogen heat treatment were calculated. Since the precipitated phases at the first and the third DTA peaks of the reduced glass (calcium titanium phosphate and calcium

pyrophosphate) were the same as those precipitated at the first and the second DTA peaks of the unreduced glass, the measurements were performed for these noted peaks.

Fig. 5a and b shows the Marotta and the Ozawa plots for calculation of the Avrami exponent before and after hydrogen heat treatment, respectively. Each plot was drawn by calculation at different heating rates of 5, 10, 15 and 20 °C/min. Table 1 shows the Avrami exponents derived from Fig. 5. As it can be seen, the Avrami exponents of the unreduced glass are near 1 at both crystallization peak temperatures. This result confirms surface crystallization mechanism at these two peak temperatures. However, the measured exponents of the reduced glass were changed to about 3, means that bulk crystallization is the prevailing mechanism of crystallization at the first and the third crystallization peak temperatures [20–22]. This difference comes from the presence of metallic silver particles in the reduced glass, which act as a nucleating agent and provide suitable sites for crystallization.

Fig. 6a and b shows the Marotta plots for calculation of activation energy for crystallization of the glass G3 before and after reduction. The results have been summarized in Table 2. According to the obtained values, activation energy for crystallization at the second peak of the unreduced glass has been increased relative to the first crystallization peak. This effect can be referred to the formation of calcium pyrophosphate at the first crystallization peak temperature, which consumes necessary constituents for precipitation of crystalline phases at the second crystallization peak temperature. In this condition, diffusion paths of constituents will be increased and will make crystallization more difficult, kinetically at the second peak temperature. As a result, the activation energy for crystallization will be increased at the second crystallization peak.

Table 1
Calculation of the Avrami exponents of glass G3.

Method	T_{C1}	T_{C2} (T_{C3})
Before hydrogen heat treatment		
Marotta	0.65	1.41
After hydrogen heat treatment		
Ozawa	2.72	3.10

Comparing the activation energies for crystallization at the first peak of the reduced and unreduced glasses shows higher activation energy of the reduced glass. However, the activation energy for the second peak of both glasses remains nearly constant. Certainly, this observation would be compatible with decreasing of the DTA crystallization peak intensities of the reduced glass. Therefore, it can be said that presence of metallic silver cannot improve kinetic of crystallization.

Accordingly, it can be concluded that metallic silver promotes crystallization, thermodynamically but cannot influence kinetic of crystallization. In fact, by reduction of silver ions and formation of silver particles, new crystal-glass interfaces are generated. Heterogeneous nucleation of crystalline phases at these interfaces decreases surface energy of the

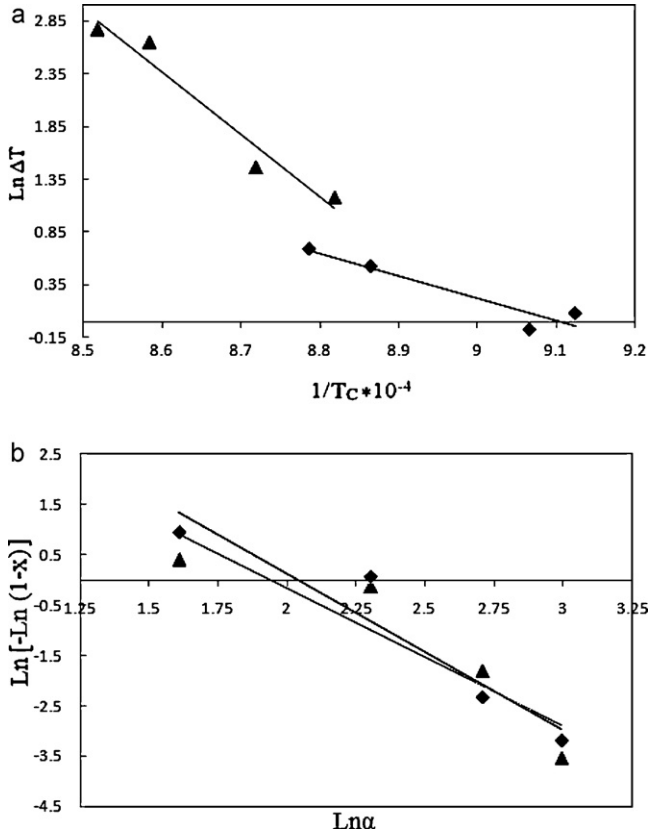

Fig. 5. Calculation of the Avrami exponents for glass G3 (a) before and (b) after hydrogen heat treatment (◆: $Ca_2P_2O_7$, ▲ $CaTi_4(PO_4)_6$).

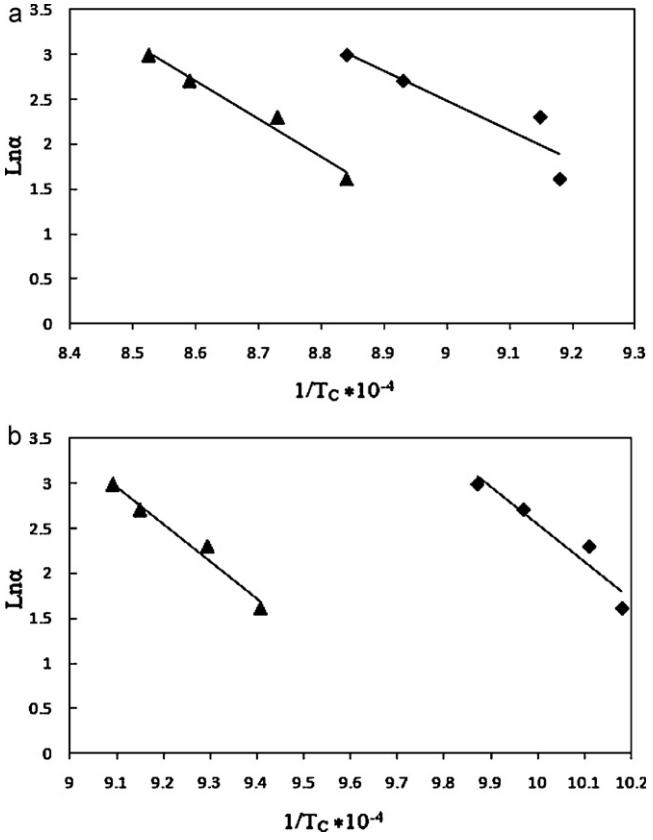

Fig. 6. Calculation of the activation energy for crystallization of glass G3 according to the Marotta method (a) before and (b) after hydrogen heat treatment (◆: $Ca_2P_2O_7$, ▲: $CaTi_4(PO_4)_6$).

Table 2
Calculation of the activation energy for crystallization of glass G3.

Method	T_{C1}	T_{C2} (T_{C3})
Before hydrogen heat treatment		
Marotta	275.7	348.7
After hydrogen heat treatment		
Marotta	345.7	345.1

extending crystalline phases (γ) which is against crystallization according to Eq. (4-1) [23]:

$$\Delta G = -\frac{4}{3}\pi r^3 \Delta G_V + 4\pi r^2 \gamma \quad (4\text{-}1)$$

ΔG, ΔG_V, γ and r are referred to the total free energy change of system, the change of free energy per unit volume resulting from crystallization, energy per unit area of surface and radius of a spherical nucleus, respectively. Therefore, formation of silver particles decreases the surface energy required for the formation of new interfaces. Furthermore, ΔG_V is influenced positively by the formation of silver particles. ΔG_V in turn can be measured from Eq. (4-2) [24]:

$$\Delta G_V = \frac{L\,\Delta T}{T_m} \quad (4\text{-}2)$$

where L is the latent heat of fusion and ΔT is the undercooling below the liquidus temperature (T_m). Exploring the DTA thermographs reveals that the undercooling temperature interval has been significantly expanded in the presence of silver particles via considerable decreasing of the crystallization peak temperatures. This modification enhances the change of free energy per unit volume and encourages crystallization, thermodynamically. Therefore, it is concluded that silver particles promotes thermodynamic of crystallization reciprocally by decreasing of surface energy and increasing of ΔG_V.

3.4. Microstructural evaluation

Fig. 7a depicts the AFM micrograph of the glass G0 after hydrogen heat treatment. As it is obvious, no special morphology can be observed in this micrograph. Fig. 7b and c shows the AFM micrographs of the glass G3 after reduction in hydrogen atmosphere. A homogeneous distribution of particles with dimensions of about 200–500 nm is detectable in these micrographs. Comparing this microstructure with smooth microstructure of glass G0, confirms the formation of silver particles in it.

The microstructures of the relevant glass–ceramics after acid leaching have been compared in Figs. 8 and 9. Prior to leaching, crystallization of the glass G_0 was performed through nucleation at 615 °C for 5 h and growth at 840 °C for 2 h. glass–ceramic G3 was obtained by heat treatment of the initial reduced glass at 712 °C for 2 h.

According to Fig. 8a and b, needle like porosities with dimensions of about 5–10 μm can be observed in the G_0

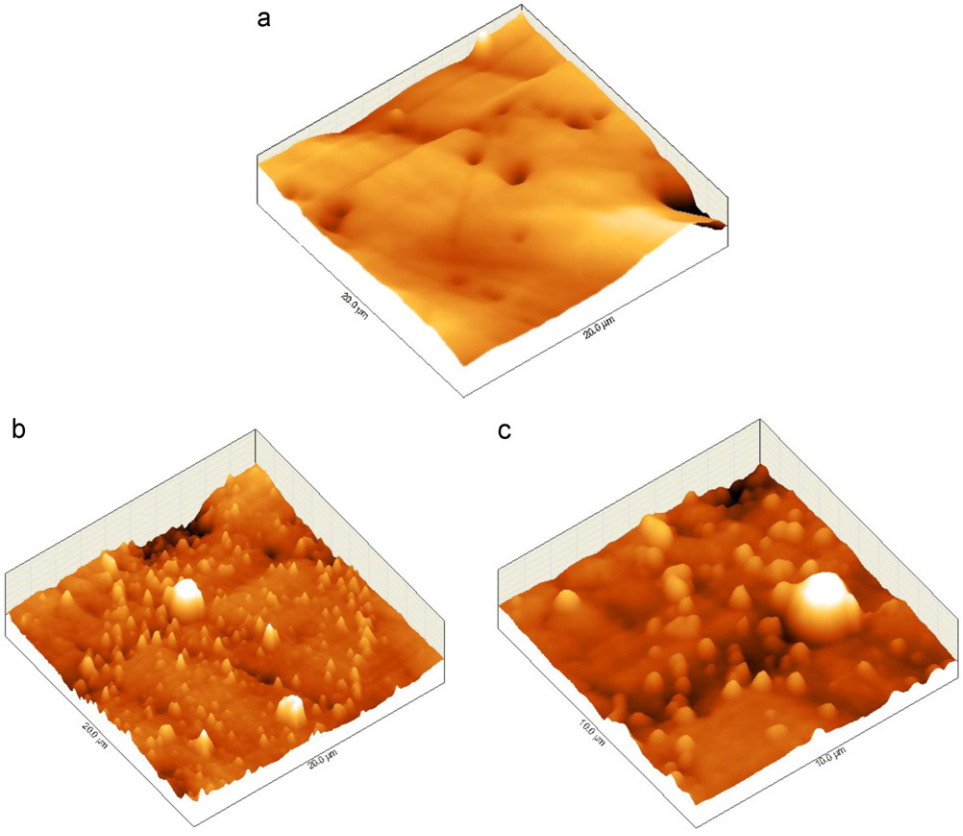

Fig. 7. AFM micrographs of bulk glasses G0 and G3 after hydrogen heat treatment (500 °C, 3 h) (a) 20 μm × 20 μm area of glass G0 (b) 20 μm × 20 μm area of glass G3 (c) 10 μm × 10 μm area of glass G3.

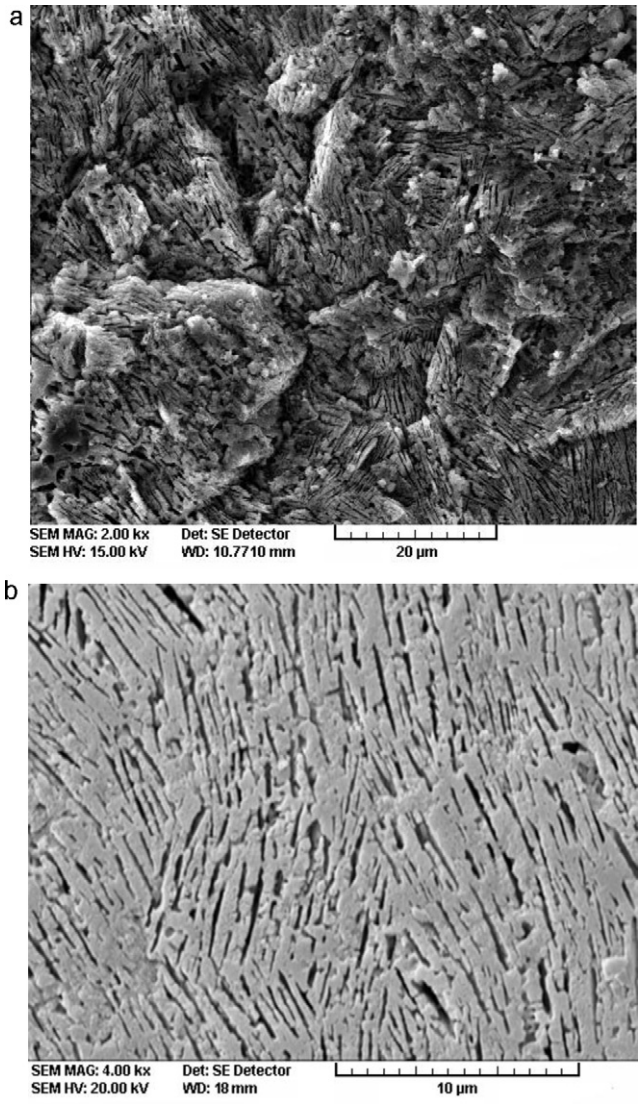

Fig. 8. SEM micrographs of heat treated glass–ceramic G0 (5 h nucleated at 615 °C, 2 h heat treated at 840 °C) after leaching: (a) 2000× magnification and (b) 4000× magnification.

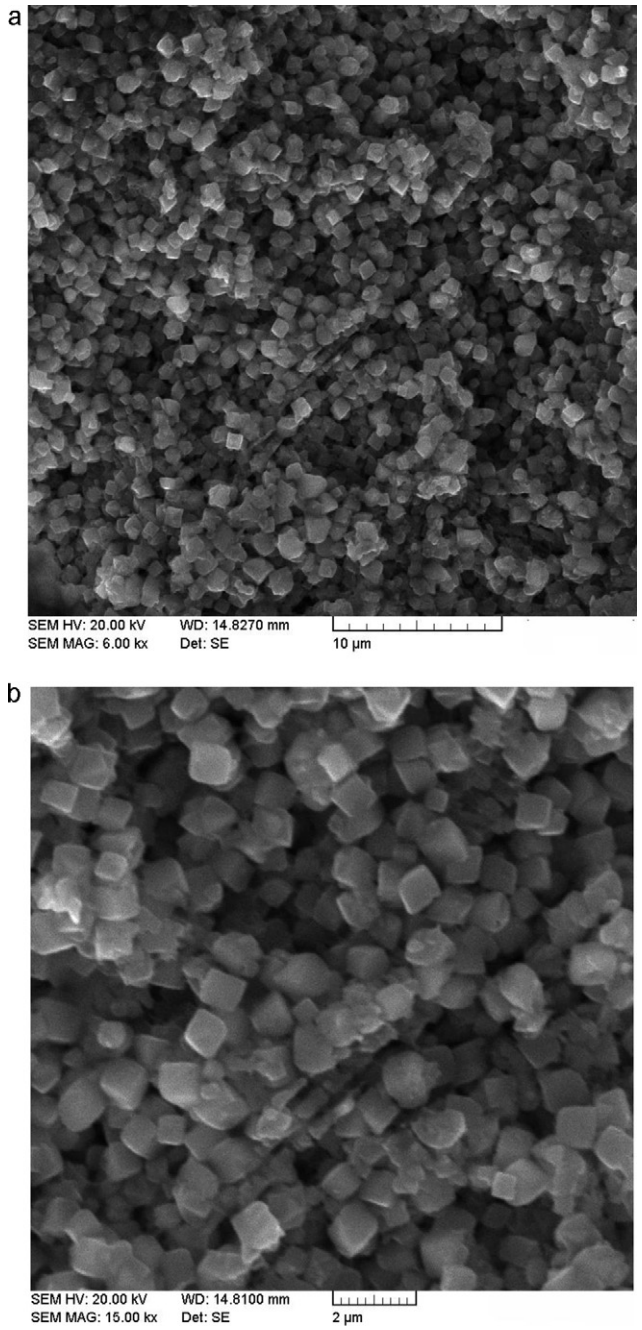

Fig. 9. SEM micrographs of glass–ceramic G3 after reducing in hydrogen, subsequent heat treatment (712 °C, 2 h) and leaching: (a) 6000× magnification and (b) 15,000× magnification.

glass–ceramic. Formation of these porosities is due to the selective dissolution of low chemically resistant calcium pyrophosphate during leaching. Fig. 9a and b shows the leached microstructure of glass–ceramic G3. In spite of the G_0 microstructure, the size and morphology of porosities are totally different in glass–ceramic G3. Although, these porosities originate again from leaching out of calcium pyrophosphate phase, however, their size has been declined to about 1–2 μm. Moreover, their morphology has been changed to near spherical. Concerning the obtained Avrami exponents of glass G3, it can be realized that metallic silver is responsible for altering the morphology from one to three dimensional states. Furthermore, nucleating role of metallic silver has increased the nucleation sites in the microstructure followed by increasing of crystallinity and decreasing of the crystal size in these sites. Decreasing the size of crystalline phases in turn decreases the size of porosities after leaching. The final porous glass–ceramics with controlled morphology and size of porosities may be suitable candidates for applications such as filtration, catalyst supports, etc.

4. Conclusions

It was found that silver modifies crystallization of CaO–Al_2O_3–TiO_2–P_2O_5 glasses in different ways. Silver ions act as a flux and improve kinetic of crystallization by decreasing the dilatometric softening point temperature and the glass viscosity. However, formation of metallic silver particles through a reducing heat treatment in hydrogen atmosphere

cannot change the kinetic of crystallization and promotes crystallization behavior, thermodynamically. Nucleating role of silver particles decreases crystallization temperatures at least 100 °C and increases crystallization sites. Leaching of silver containing glass–ceramics leaves reduced in size porosities with near spherical morphology rather than silver free porous structure with needle like larger porosities. Porous structure of final products can be appropriate for applications which demand fine porous structure with controlled pore morphology.

References

[1] H. Hosono, Z.H. Zhang, Y. Abe, Porous glass–ceramics in the $CaO–TiO_2–P_2O_5$ System, J. Am. Ceram. Soc. 72 (9) (1989) 1587–1590.

[2] H. Hosono, Y. Abe, Porous glass–ceramics composed of a titanium phosphate crystal skeleton: a review, J. Non-Cryst. Solids 190 (2–3) (1995) 185–197.

[3] H. Hosono, Y. Abe, Fast lithium conducting glass–ceramics in the $Li_2O–CaO–TiO_2–A1_2O_3–P_2O_5$ system, Solid State Ionics 44 (3–4) (1991) 293–297.

[4] H. Hosono, Y. Abe, Porous glass–ceramics with a skeleton of the fast-lithium conducting crystal $Li_{1+x}Ti_{2-x}(PO_4)_3$, J. Am. Ceram. Soc. 75 (10) (1992) 2862–2864.

[5] T. Kasuga, H. Kume, Y. Abe, Porous glass–ceramics with bacteriostatic properties in silver-containing titanium phosphates: control of release of silver ions from glass–ceramics into aqueous solution, J. Am. Ceram. Soc. 80 (3) (1997) 777–780.

[6] T. Kasuga, H. Nakamura, K. Yamamoto, M. Nogami, Y. Abe, Microporous materials with an integrated skeleton of $AgTi_2(PO_4)_3$ and $Ti(HPO_4)_2·2H_2O$ crystals, Chem. Mater. 10 (11) (1998) 3562–3567.

[7] K. Yamamoto, Y. Abe, Microporous glass–ceramics in NASICON-type copper (II) titanium phosphate, J. Am. Ceram. Soc. 81 (8) (1998) 2201–2204.

[8] K. Yamamoto, Y. Abe, Enhanced catalytic activity of microporous glass–ceramics with a skeleton of NASICON-type copper (I) titanium phosphate crystal, Mater. Res. Bull. 35 (2) (2000) 211–216.

[9] M. Kord, V.K. Marghussian, B. Eftekhari Yekta, A. Bahrami, Effect of ZrO2 addition on crystallization behavior, porosity and chemical–mechanical properties of a $CaO–TiO_2–P_2O_5$ microporous glass–ceramic, Mater. Res. Bull. 44 (8) (2009) 1670–1675.

[10] Y. Daiko, H. Yajima, T. Kasuga, Preparation of porous titanium phosphate glass–ceramics for NH_3 gas adsorption with self-cleaning ability, J. Eur. Ceram. Soc. 28 (1) (2008) 267–270.

[11] S. Banijamali, A.R. Aghaei, B. Eftekhari Yekta, Improving glass-forming ability and crystallization behavior of porous glass–ceramics in $CaO–Al_2O_3–TiO_2–P_2O_5$ system, J. Non-Cryst. Solids 356 (31–32) (2010) 1569–1575.

[12] S. Banijamali, B. Eftekhari Yekta, A.R. Aghaei, The effect of ionic and metallic silver on the crystalline phases developed in $CaO–Al_2O_3–TiO_2.P_2O_5$ glasses, J. Non-Cryst. Solids, in press, doi:10.1016/j.jnoncrysol.2011.09.026.

[13] F. Branda, A. Buri, A. Marotta, S. Saiello, Kinetic of crystal growth in $Na_2O–2SiO_2$ glass: a DTA study, Thermochim. Acta 77 (1–3) (1984) 13–18.

[14] I. Dyamant, E. Korin, J. Hormadaly, Non-isothermal crystallization kinetics of $La_2CaB_{10}O_{19}$ from glass, J. Non-Cryst. Solids 357 (7) (2011) 1690–1695.

[15] M. Erol, S. Küçükbayrak, A. Ersoy-Meriçboyu, Influence of particle size on the crystallization kinetics of glasses produced from waste materials, J. Non-Cryst. Solids 357 (1) (2011) 211–219.

[16] M.A. Mousa, Imran, Crystallization kinetics, glass transition kinetics, and thermal stability of $Se_{70-x}Ga_{30}In_x$ (x = 5, 10, 15, and 20) semiconducting glasses, Physica B 406 (3) (2011) 482–487.

[17] B. Deb, A. Ghosh, Crystallization kinetics in selenium molybdate molecular glasses, Europhys. Lett. 95 (2) (2011) 26002.

[18] S.S. Das, P. Singh, DSC studies on sodium phosphate glasses doped with chlorides of Cd, Co and Ag, J. Therm. Anal. Calorim. 78 (3) (2004) 731–738.

[19] W. Holand, G. Beall, Glass–Ceramic Technology, American Ceramic Society, OH, 2002, p. 178.

[20] I.W. Donald, Crystallization kinetics of a lithium zinc silicate glass studied by DTA and DSC, J. Non-Cryst. Solids 345–346 (2004) 120–126.

[21] A. Arora, A. Goel, E.R. Shaaban, K. Singh, O.P. Pandey, J.M.F. Ferreira, Crystallization kinetics of $BaO–ZnO–Al_2O_3–B_2O_3–SiO_2$ glass, Physica B 403 (10–11) (2008) 1738–1746.

[22] M. Çelikbilek, A.E. Ersundu, N. Solak, S. Aydin, Crystallization kinetics of the tungsten–tellurite glasses, J. Non-Cryst. Solids 357 (1) (2011) 88–95.

[23] W. Holand, G. Beall, Glass–Ceramic Technology, American Ceramic Society, OH, 2002, p. 40.

[24] J.E. Shelby, Introduction to glass science and technology, R. Soc. Chem. (1997) 13.